A Case Study of Mesoscale Convective System Reorganization off of the West Coast of Africa

SONNY KREMIN*

National Weather Center Research Experiences for Undergraduates Program
Norman, Oklahoma,
St. Cloud State University
St. Cloud, Minnesota

SHUN-NAN WU AND NAOKO SAKADEA
School of Meteorology, University of Oklahoma
Norman, Oklahoma

ABSTRACT

Previous studies on the land-to-ocean transitions of Mesoscale Convective Systems (MCSs) concluded that MCSs tend to weaken or dissipate post-transition. On the 14th September 2022 a MCS transitioning off of the West African coast initially weakened and then later rapidly re-intensified over the Tropical North Atlantic. Precipitation data from the Integrated Multi-satellite Retrievals for GPM (IMERG) and Tracked IMERG Mesoscale Precipitation System (TIMPS) is used to track the position and strength of the system as it transitioned offshore. Dropsonde data from research flight five of the Convective Processes EXperiment–Cabo Verde (CPEX-CV) campaign is analyzed to determine what environmental factors caused this redevelopment over the Atlantic. Boundary layer moisture, 700 hPa winds, and other environmental factors are analyzed and reveal that rapid strengthening of the African Easterly Jet and enhanced moisture ahead of the system are likely factors that caused the system's re-development.

1. Introduction

A Mesoscale Convective System (MCS) is typically defined as an organized complex of thunderstorms, lasting for several hours, with an area of continuous precipitation on the scale of approximately 100 km. MCSs have been recognized as a significant source of precipitation in the tropics, producing approximately 50% to 60% of all precipitation in the tropics (Feng et al. 2021). In addition, tropical MCSs can also develop into tropical cyclones (GRAY 1968). These impacts have caused interest in the origins and development of tropical MCSs, particularly in the region of the land-sea transition of West Africa, where much of their development remains unclear.

Previous studies using data collected by the NASA African Monsoon Multidisciplinary Analyses (NAMMA) campaign have concluded that MCS tend to weaken or dissipate after transitioning to a maritime environment, depending on their initial strength on land and the thermodynamic properties of the coastal environment (Klotz and Kucera 2012; DeLonge et al. 2010; Guy et al. 2011). These studies are limited by the fact that observations used from this campaign were limited to the immediate coastal region and did not use any in-situ data sampling the maritime environment. This left many questions about the development of convective systems over the Eastern Atlantic for future research.

The Convective Processes EXperiment - Cabo Verde (CPEX-CV), was a NASA campaign aimed at studying the interactions and dynamics of the atmosphere in the Eastern Atlantic during September 2022. The campaign utilized the NASA DC-8 Airborne Science Laboratory, which was outfitted with a dropsonde launch tube and a suite of remote sensing instruments. On the fifth flight of this campaign a MCS was observed that weakened after transitioning off of the West African coast but then re-organized and re-intensified into a squall line MCS. This re-development leads to questioning whether system development post-transition is more complex than previously thought.

This study aims to understand what environmental factors caused this offshore re-organization. A few hypotheses presented are that increased moisture from the african monsoon flow encouraged re-development, or potentially an interaction with the African Easterly Wave (AEW) associated with this MCS caused the re-development.

*Corresponding author address: Sonny Kremin, Department of Atmospheric and Hydrologic Sciences, St. Cloud State University, St. Cloud, MN 56301.
E-mail: sonnykremin@gmail.com

2. Data & Methods

a. Global Satellite Precipitation Retrieval

NASA's Integrated Multi-satellite Retrievals for GPM (IMERG) is an algorithm that combines retrievals of Global Precipitation Measurement (GPM) observations with other polar and geostationary satellite data to estimate precipitation over the earth from 60° N to 60° S in 0.1° bins at 30-minute increments (Huffman et al. 2019). For our study, this dataset is primarily used in conjunction with a tracking algorithm to determine the position of MCSs and track their development.

b. MCS Tracking Algorithm

For identifying and tracking MCS, the Tracked IMERG Mesoscale Precipitation System (TIMPS) was utilized (Rajagopal et al. 2023). The TIMPS algorithm applies a modified version of the Forward in Time (FiT) tracking algorithm to smoothed and thresholded IMERG precipitation data. IMERG data is smoothed with a moving 5 grid cell average, a 1 mm/hr threshold is applied, and systems meeting the FiT thresholds for MCSs are tracked when their centers are at least 20 grid cells apart. TIMPS produces two sets of data, a geographical tracking file and a system file containing information on a particular tracked system. From these two files, we analyzed system position, system area, average and maximum rainfall rates, and volumetric rain rate.

c. DC-8 Flight Track

The flight on the 14th of September 2022 was the 5th flight of the CPEX-CV campaign. On this flight, 30 dropsondes were released, 5 of which did not collect data due to technical issues with the dropsonde launch system (Thornhill 2023). Of the 25 dropsondes that returned data, only 4 were in the pre-system environment. **Fig. 1** shows the flight path of the DC-8 plotted as a black line, underlied with IMERG mean precipitation rate, the white dots mark the locations of successfully deployed dropsondes with unsuccessful dropsondes marked in red. The region labeled "a." in blue is what we will call pre-system environment A (**env. A**) and the region labeled "b." in red is what will be called pre-system environment B (**env. B**). The dropsondes circled in **env. A** & **B** are the only dropsondes that were launched in the pre-system environment. For the analysis in this study, we will associate a MCS located north of the MCS of interest that did not redevelop with **env. A** (**MCS A**) and the MCS of interest with **env. B** (**MCS B**) as **MCS A** dissipated after propagating to **env. A** and **MCS B** redeveloped after propagating to **env. B**, therefore we can directly compare **env. A** & **B** to determine what may have influenced the development of **MCS B**.

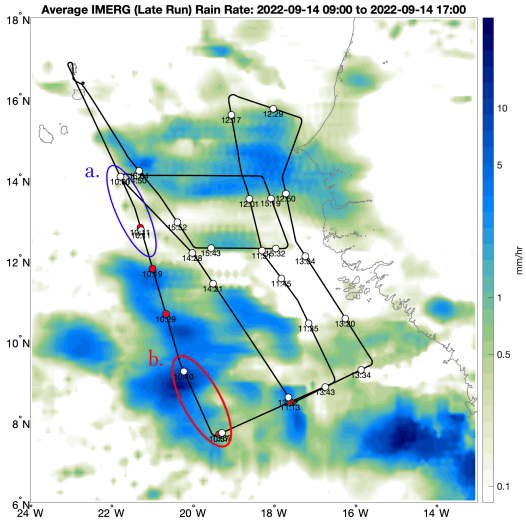

FIG. 1. The IMERG mean rain rate from 9:00-17:00 UTC 14/09/2022 is shaded in blue-green with the unit of mm hr^{-1}. The flight path of the DC-8 is plotted as a black line. The dots with time in UTC under them mark the location and time of dropsonde launches with red dots indicating dropsondes with no data. The region circled in blue is **env. A** with precipitation to the east being created by **MCS A**. The region circled in red is **env. B** with precipitation in the region being created by **MCS B**.

d. Dropsonde Data

Dropsonde data collected during the CPEX-CV campaign was analyzed by calculating CAPE and CIN with MetPy calc, and plotting the positions of the dropsondes with calculated variables of the environment. As the dropsonde data is not interpolated, to get estimated values at designated pressure levels, variables representative of select levels were derived by taking the average of all samples collected within $\pm$ 5 hPa of the desired pressure level. Variables used in the analysis were GPS-estimated wind, dry bulb temperature, relative humidity, dewpoint, and mixing ratio. CAPE and CIN were calculated in the layer between 1000 hPa and 500 hPa to allow for comparable values across soundings. Vertical wind shear was computed using the difference of winds between the 1000 hPa and 850 hPa levels for the boundary layer shear and the difference between 850 hPa and 600 hPa winds for the mid-level shear. Boundary layer moisture was derived by averaging the mixing ratio between 1000 and 850 hPa.

3. Results

a. IMERG & System Tracking

Mapped plots of IMERG precipitation estimates were used to analyze the position, structure, and rainfall rates of **MCS B** and can be seen in **Fig. 2**. The system was considered to initialize at 10:30z 13th September 2022,

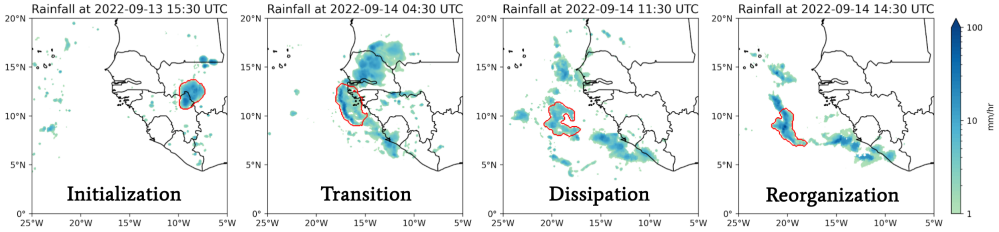

FIG. 2. General development of **MCS B** with time progressing from left to right. **MCS B** is circled in red, with IMERG 30 minute precipitation rate shaded in blue-green.

over South Western Mali and began to propagate westward. As it propagated offshore it developed into a squall line at around 2:30z 14th September 2022. The deep convection of the system began to dissipate and become primarily stratiform until it re-organized into a squall line at 14:00 UTC. It then continued to dissipate into stratiform precipitation at 17:30 UTC.

An analysis of maximum precipitation rate, average precipitation rate, volumetric rain rate, and system area was done using the TIMPS system file and a graph of these values can be seen in **Fig. 3**. For the purposes of this study, we are only interested in the system's development on the 14th of September.

Analyzing the maximum precipitation rate of the system, there is an initial peak of about 74 mm hr^{-1} at 5:30 UTC, associated with the propagation of the initial squall line off of the West African coast.The system weakens at 11z and the maximum precipitation rate of the system decreased to only 18 mm hr^{-1}, while the system re-organized itself into squall line at 14:30 UTC, with the largest peak of 110 mm hr^{-1}. The mean rain rate shows similar evolution with lower intensities of 6, 3, and 8 mm hr^{-1}, with a difference of peak times for second and third peak, at 10:30 UTC and 14:00 UTC respectively. The volumetric rain rate had two notable peaks of 708 m km^2 hr^{-1} and 580 m km^2 hr^{-1} at 5:30 UTC and 16:00 UTC respectively. System area did not display particular significance but decreased overall as the system progressed.

Overall, the evolution of rainfall rates associated with MCSs is consistent with mapped plots of IMERG, suggesting that the MCS experienced the re-organization/re-intensification after propagating offshore. Thus, the next section analyzes the dropsonde data to examine the environmental factors that helped MCS re-organization.

b. Dropsonde Maps

A series of variables from dropsonde data were mapped out in the offshore region of West Africa to examine the pre-storm environment that helped MCS re-organization.

1) LOW-LEVEL CAPE

Low-level CAPE was analyzed to account for differences in static stability that may have had an impact on the development of the systems, **Fig. 4** a plot of 1000-500 hPa CAPE with 1000 hPa wind was made. **Env. A** had low level CAPE varying from 503 J kg^{-1} to 434 J kg^{-1} with **env. B** varying from 503 J kg^{-1} to 354 J kg^{-1}. The post storm environment for radiosondes not deployed in convective systems had CAPE varying from 286 J kg^{-1} to -68 J kg^{-1}. This suggests that although differences in CAPE did not have a large influence on the development of the systems, a certain amount of CAPE is necessary for the MCS development.

2) ACTIVITY OF AFRICAN EASTERLY WAVE

The 700 hPa level was analyzed to identify the location of an AEW known to have propagated offshore during the day of the event (Bucci et al. 2023). **Fig. 5** shows no signature of an AEW trough, but there are strong 50-30 kt winds near the coast, indicating the presence of the African Easterly Jet (AEJ). As time progresses, there is an increase in strength and extent of the jet. The meridional extent of the AEJ is approximately 14°-10° N and it extends out to 20° W from the coast. The intensification can be seen as the increase in wind speeds of soundings later in the flight such as the 14:16 & 15:40 UTC soundings (The closest magenta and brown soundings). Although the dropsonde data cannot represent the entire AEJ strengthening event, this rapid intensification of AEJ is consistent with a Saharan Air Layer (SAL) outbreak over Africa observed during the flight.

3) VERTICAL WIND SHEAR

Shear was analyzed to compare **env. A** to **env. B** (**Fig. 6**), as moderate shear has been shown to enhance the development of MCSs (Chen et al. 2023). The shear in **env. A** was quite weak with very little to no low-level shear and only moderate mid-level shear. The shear in **env. B** by comparison was greater than the shear in **env. A**, being more moderate in the lower and mid levels. The shear in the post-system environment is very high in the low levels due to the AEJ.

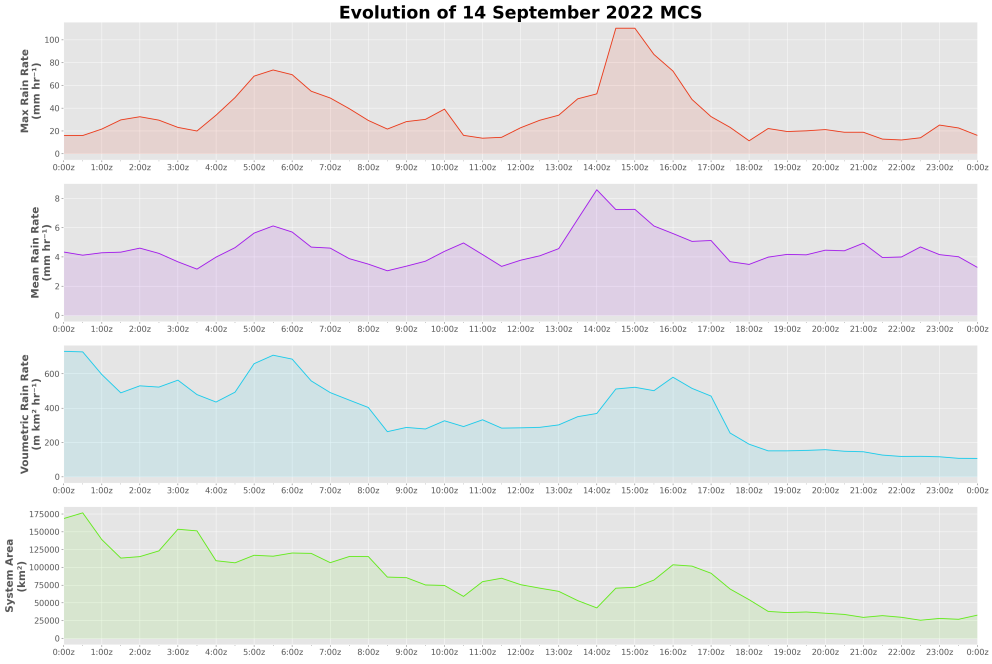

FIG. 3. Time series of the maximum rain rate, mean rain rate, volumetric rain rate, and system area of **MCS B** with time in UTC.

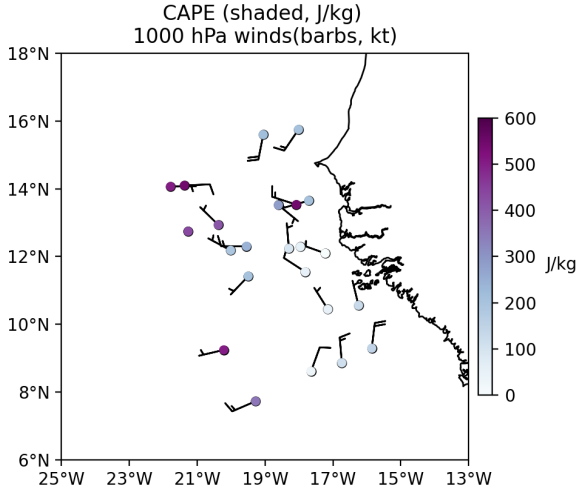

FIG. 4. Plot of all dropsonde positions with CAPE shaded and 1000 hPa winds plotted with wind barbs.

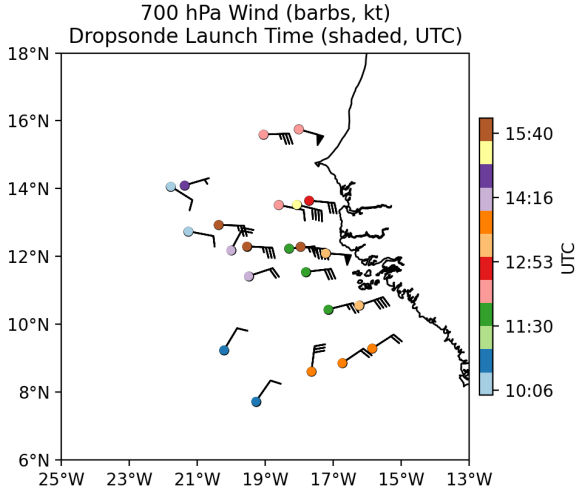

FIG. 5. Same as Fig. 4 but time in UTC is shaded and wind barbs are from the 700 hPa level. Dropsonde launch times range from 10:00 UTC to 15:52 UTC.

4) LOW LEVEL MONSOON

The low level winds and mixing ratio were analyzed to compare the boundary layer moisture available in both environments. The mixing ratio in **env. B** was much higher than in **env. A** (**Fig. 7**), being around 17 g kg^{-1} compared to about 15 g kg^{-1}. This makes **env. B** more conducive to MCS maintenance. This higher mixing ratio is likely due to the presence of a seasonal monsoon south of the West African coast indicated by the southwesterly winds in the environment. In the post-system environment, an intrusion of the SAL off the central coast of West Africa can be seen as low boundary layer mixing ratios of around 12 g kg^{-1}.

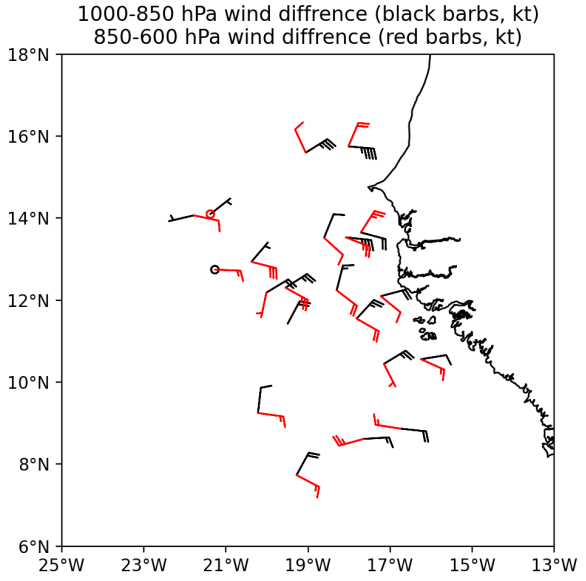

FIG. 6. Plot of all dropsonde positions with 1000 & 850 hPa wind difference plotted with black wind barbs and 850 & 600 hPa wind difference plotted with red wind barbs.

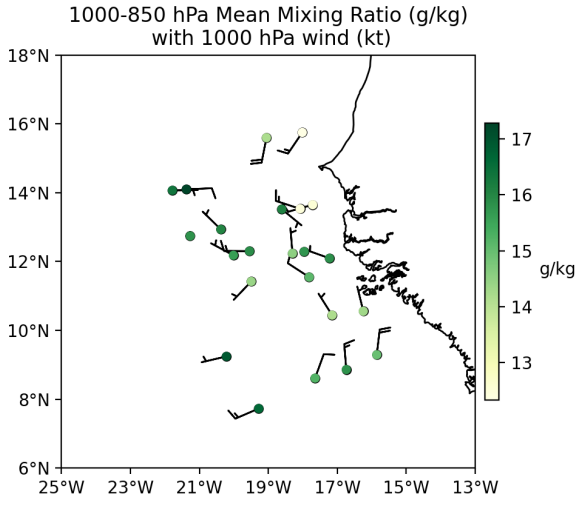

FIG. 7. Same as Fig. 4 but with 1000 to 850 hPa mean boundary layer mixing ratio shaded in yellow-green.

4. Discussion & Conclusion

IMERG precipitation data and dropsonde data from the CPEX-CV campaign were analyzed to find what environmental factors likely caused the system to redevelop over the ocean.

Analysis of CAPE was difficult as the DC-8 flew anywhere from 400-490 hPa making full sounding CAPE incalculable. Inversions in the upper levels may have caused variances in CAPE that we would not be able to detect using this data. Analysis of the low-level CAPE from 1000-500 hPa revealed that CAPE was likely not a significant factor in the redevelopment of the system, due to there being little difference in **env. A** to **env. B**.

The analysis of the 700 hPa winds did not reveal an AEW trough, but did reveal the presence and intensification of the AEJ at around 14:00 UTC after which time there was a rapid increase in the maximum rain rate of the system indicated by the TIMPS tracking file, making the AEJ the most likely factor to cause the redevelopment. The possible mechanism behind this redevelopment may have been the AEJ enhancing the rear-inflow jet of the MCS, causing the upshear tilted updraft to tilt more vertically, enhancing deep convection.

An analysis of the environmental shear was done and revealed that in the pre-system environment shear in **env. B** was stronger than in **env. A**, possibly aiding in the redevelopment of the system. Although this shear may be due to the close placement of the dropsondes to the MCS sampling the system shear. Shear in the post-system environment had high low-level shear caused by the presence of the AEJ, mid-level shear remained relatively low in the post-system environment.

The boundary layer mean mixing ratio was analyzed in the pre-system environment to determine if anomalous amounts of moisture were present. **Env. A** had a higher mean mixing ratio of 17 g kg^{-1} which would have been sufficient to maintain the convection seen in the MCS. Moisture in the post-system environment was moderate at 15 g kg^{-1} except near the central West African coast where a SAL intrusion caused mixing ratios to be around 12 g kg^{-1}.

In summary, we found that the environment ahead of the re-organizing MCS demonstrated greater low-level moisture and moderate vertical wind shear, indicating the prevailing monsoonal flow and accelerating AEJ's critical role in the development of the MCS. Future work could look at finding more events similar to this one and attempting to build a climatology of these events, other work could involve model simulations testing the theory of AEJ's enhancement of the MCS's rear-inflow jet.

Acknowledgments. The corresponding author would like to thank the directors of the Real-World Research Experiences for Undergraduates (REU) at the National Weather Center, Alex Marmo and Dr. Daphne LaDue for organizing the REU, and support thru-out the program. This material is based upon work supported by the National Science Foundation under Grant No. AGS-2050267.

References

Bucci, L., L. Alaka, A. Hagen, S. Delgado, and J. Beven, 2023: Tropical cyclone report: Hurricane Ian. National Hurricane Center, URL https://www.nhc.noaa.gov/data/tcr/AL092022_Ian.pdf, 72 pp.

Chen, X., L. R. Leung, Z. Feng, and Q. Yang, 2023: Environmental controls on mcs lifetime rainfall over tropical oceans. *Geophysical Research Letters*, **50 (15)**, e2023GL103 267, doi:https://doi.org/10.1029/2023GL103267.

DeLonge, M. S., J. D. Fuentes, S. Chan, P. A. Kucera, E. Joseph, A. T. Gaye, and B. Daouda, 2010: Attributes of mesoscale convective systems at the land-ocean transition in senegal during nasa african monsoon multidisciplinary analyses 2006. *Journal of Geophysical Research: Atmospheres*, **115 (D10)**, doi:https://doi.org/10.1029/2009JD012518.

Feng, Z., and Coauthors, 2021: A global high-resolution mesoscale convective system database using satellite-derived cloud tops, surface precipitation, and tracking. *Journal of Geophysical Research: Atmospheres*, **126 (8)**, e2020JD034 202, doi:https://doi.org/10.1029/2020JD034202.

GRAY, W. M., 1968: Global view of the origin of tropical disturbances and storms. *Monthly Weather Review*, **96 (10)**, 669 – 700, doi:10.1175/1520-0493(1968)096⟨0669:GVOTOO⟩2.0.CO;2.

Guy, N., S. A. Rutledge, and R. Cifelli, 2011: Radar characteristics of continental, coastal, and maritime convection observed during amma/namma. *Quarterly Journal of the Royal Meteorological Society*, **137 (658)**, 1241–1256, doi:https://doi.org/10.1002/qj.839.

Huffman, G., E. Stocker, D. Bolvin, E. Nelkin, and J. Tan, 2019: GPM IMERG Final Precipitation L3 Half Hourly 0.1 degree x 0.1 degree V06. Goddard Earth Sciences Data and Information Services Center (GES DISC), accessed 28 May 2024, doi:10.5067/GPM/IMERG/3B-HH-L/06.

Klotz, B. W., and P. Kucera, 2012: Observations of coastally transitioning west african mesoscale convective systems during namma. *International Journal of Geophysics*, **2012 (1)**, 438 706, doi:https://doi.org/10.1155/2012/438706.

Rajagopal, M., J. Russell, G. Skok, and E. Zipser, 2023: Tracking mesoscale convective systems in imerg and regional variability of their properties in the tropics. *Journal of Geophysical Research: Atmospheres*, **128 (24)**, e2023JD038 563, doi:https://doi.org/10.1029/2023JD038563.

Thornhill, L., 2023: CPEX-CV dropsonde data. NASA Langley Atmospheric Science Data Center Distributed Active Archive Center, URL https://asdc.larc.nasa.gov/project/CPEX-CV/CPEXCV-Dropsondes_1, doi:10.5067/ASDC/SUBORBITAL/CPEXCV-DROPSONDES_1.